7

Studies on Crystals of Intact Bacterial Ribosomal Particles

A. YONATH, M. A. SAPER, and H. G. WITTMANN

Introduction

A reliable molecular model for ribosomes is essential for the understanding of their role in protein biosynthesis. In parallel to extensive chemical, physical, immunological, and genetic studies, we have extended our efforts toward the use of X-ray crystallography and three-dimensional reconstruction of electron micrographs. These techniques are very powerful since they offer direct structural information. Their application depends on the availability of crystalline materials.

Because of the complexity, enormous size, instability, and flexibility of ribosomes, there have been many doubts whether crystal growth is at all possible. Nevertheless, natural periodic organizations of ordered arrays of ribosomal particles have been reported previously. In particular, under special conditions (such as suboptimal temperatures, lack of oxygen, hibernation, etc.) the ribosomes of several eukaryotic species (lizard, chicken, amoeba, and human) associate with each other in vivo to form helices and two-dimensional layers (Kress et al., 1971; Lake and Slayter, 1972; Taddei, 1972; Unwin and Taddei, 1977; Barbieri, 1979; Unwin, 1979; O'Brien et al., 1980; Kühlbrandt and Unwin, 1982; Milligan and Unwin, 1982). Electron microscopy and image reconstruction studies of some of these ordered forms have revealed useful low-resolution information about the modes of packing, the interactions between the particles, the outer contour of the ribosomes, and the inner distribution of their components. However, the quality of the results obtained from such studies is limited by the very nature of the systems. The organization of the sheets is induced by cellular effects and is expressed in only one or two dimensions. Thus, the only diffraction techniques that can be applied are image reconstruction

B. Hardesty et al. (eds.), *Structure, Function, and Genetics of Ribosomes*

from electron micrographs and "powder" patterns. These techniques have many merits but also severe limitations.

Our efforts are directed at growing three-dimensional crystals of ribosomes from prokaryotes. These particles are smaller and have been characterized in much greater detail than those from eukaryotes. Also they can be produced in high purity and large quantity and provide a system for crystallization that is independent of in vivo events. We have developed in vitro crystallization procedure for ribosomal particles. So far we have obtained three-dimensional crystals of whole ribosomes from *Escherichia coli* (Wittmann et al., 1982) as well as of the large ribosomal subunits from *Halobacterium marismortui* (Shevack et al., 1985) and from *Bacillus stearothermophilus* (Yonath et al., 1980, 1982a, b, 1983a, b; Yonath, 1984; Yonath et al., in press, Wittmann and Yonath, 1985). From the latter we were also able to produce reproducibly two-dimensional sheets and helical organizations (Yonath et al., 1983a; Arad et al., 1984a, b; Leonard et al., 1984). Large crystals of the 50S subunits from *B. stearothermophilus* and *H. marismortui* are suitable for X-ray crystallographic structure analysis (Yonath et al., 1984, 1986; Saper et al., 1985; Shevack, Shoham, Saper, Wittmann, and Yonath, unpublished observations). Some of the three-dimensional crystals and the two-dimensional sheets have been studied by electron microscopy and image reconstruction techniques (Leonard et al., 1981, 1982, 1984; Yonath, 1984; Arad et al., 1984a, b; Wittmann and Yonath, 1985).

Ribosomes from *H. marismortui* are of special interest since they are stable and active at high salt concentrations. Their expected structure should not only contribute to the understanding of the process of protein biosynthesis but also could be used for comparative structural and functional studies. This may provide a tool for the understanding of the nature of protein–nucleic acid interactions at extremely high salt concentrations, a fundamental problem in molecular biology, for which few data are currently available. Also, since this is an archaebacterium, the comparison of the structure of its ribosome with that of the ribosome from eubacteria may shed light on basic points in evolution.

Results

In general, we find that only active preparations of ribosomes yield crystals, but the quality of the crystals depends strongly in a yet uncharacterized manner on the ribosome preparation. Owing to the intricate nature of the particles, the exact conditions for growing large, mechanically stable, and well-ordered crystals must still be slightly varied for each ribosomal preparation. Furthermore, for each such preparation, better crystals are obtained from fresh, never frozen active particles. Therefore, we screened bacterial sources and strains for their capability to produce ribosomes

in the quantity and quality required for a careful refinement of the crystallization conditions as well as for the growth of many crystals needed for data collection. It was also found that there is a correlation between the quality of the crystals and the integrity of the rRNA. This chain can be slightly cleaved without impairing the activity and the crystallizability of the particles.

50S Ribosomal Subunits from *Bacillus stearothermophilus*

Crystals from the large ribosomal subunits from two strains (799 and NCA) of *B. stearothermophilus* have been used for single crystal X-ray crystallographic studies with synchrotron radiation. Large crystals, which may reach a size of $1.5 \times 0.25 \times 0.15$ mm (Fig. 7.1), grow in the presence of alcohol mixtures as long pointed needles directly in X-ray capillaries (Yonath et al., 1982b, 1984). Since most of them grow with one of their faces adhering to the walls of the capillaries, it is possible to irradiate them without removing the original growth solution. Experiments prove that crystals kept in growth solution last significantly longer in the X-ray beam and rarely develop as many cracks as crystals that have been slightly dried. Despite the increase in scattering, X-ray diffraction patterns extend to higher resolution, and data of better quality can be collected. Although most of the crystals grow so that their long axes lay parallel to the capillary axis, a fair number of them grow in different directions. Thus, in spite of the overcrowding of crystals that often imposes difficulties in finding solitary crystals in proper orientations, we were able to obtain diffraction

Figure 7.1. a. Crystals of the 50S ribosomal particles from *B. stearothermophilus*, grown in an X-ray capillary by vapor diffusion against 14–17% ethyleneglycol and 14–17% methanol at pH 8.4–9.2. Bar length, 0.2 mm. b. A 1.5° rotation X-ray diffraction pattern of the 680 Å × 920Å major zone, obtained from a crystal similar to that shown in (a) with synchrotron beam at X11/DORIS (EMBL/DESY), under parasitic conditions at about 5 GEV and 25 mA, with 0.20 mm aperture, for 20 min at −2 °C. Crystal to film distance, 135 mm. Systematic absences along the marked major axis indicate a twofold screw axis. Two different "spot shapes" can easily be detected. These result from exposure of a second crystal, within the same capillary, approximately perpendicular to the first one. c. The central part of a still X-ray diffraction pattern of crystals of strain 799 grown from 19% ethyleneglycol and 15% methanol at pH 8.4. The pattern was obtained with synchrotron beam at X11/DORIS (EMBL/DESY), under parasitic conditions at about 5.3 GEV and 25 mA, with 0.2 mm aperture, for 15 min at 12 °C. Crystal to film distance, 125 mm. It contains features with spacings of 240 ± 2 Å and 360 ± 2 Å (see Table 7.1, forms 1–3 and 2D sheets). d. Electron micrographs of two positively stained sections, approximately perpendicular to each other of an embedded crystal similar to that shown in (a) and their diffraction patterns. Two possibilities of unit cell assignment for the loosely packed section are marked: dashed lines for the smaller, pseudo-hexagonal one, full for the large, pseudo-orthorhombic one. Bar length, 1000 Å.

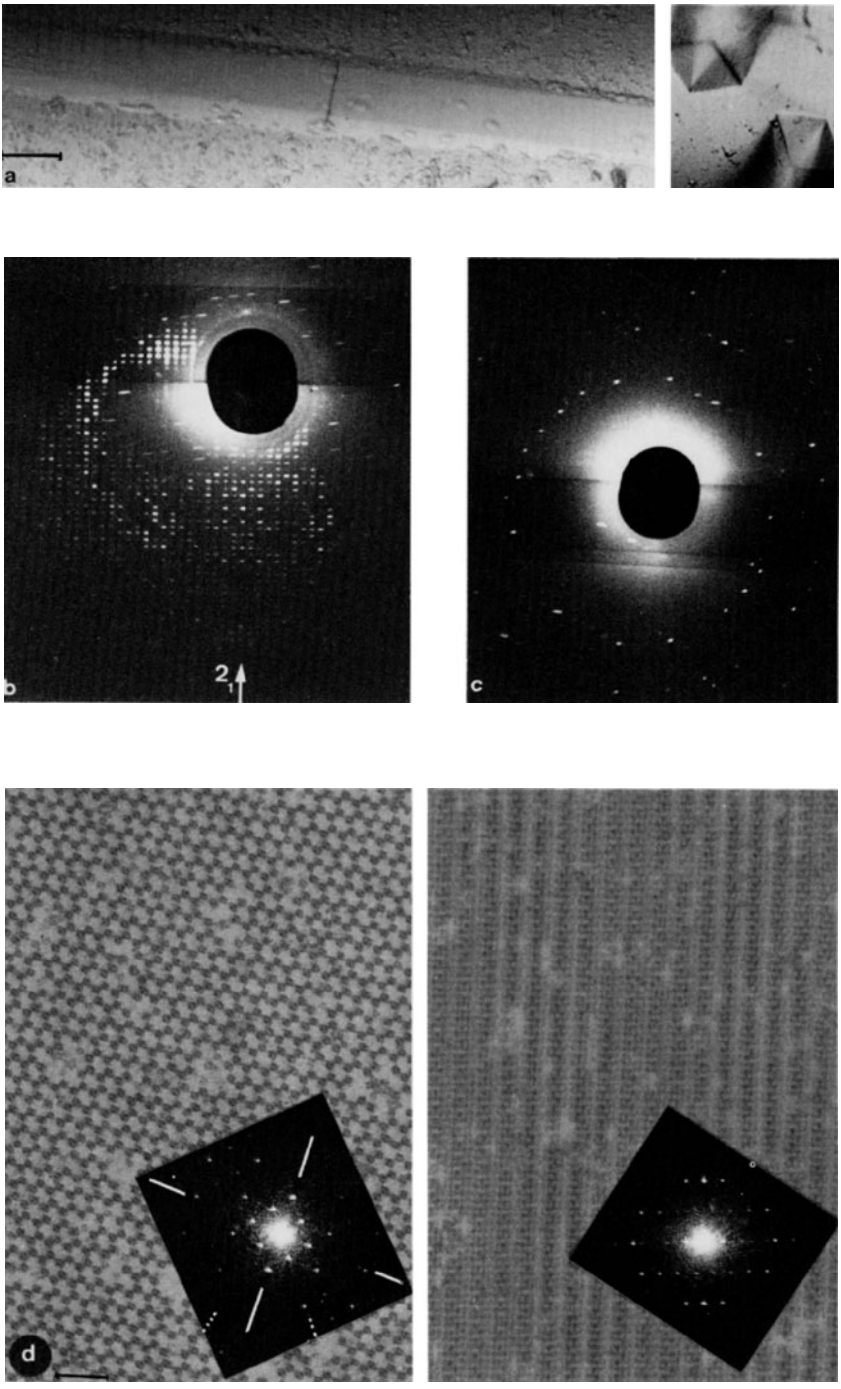
a
b
2_1
c
d

patterns from all of the zones without manipulating the crystals. In their natural growth medium, the crystals are adequately stable for 6 to 8 weeks. Any handling of the crystals, such as removing or reorienting the crystals or replacing the growth medium with a different solution, is virtually impossible in our system. Once handled, the crystals remain intact for less than 2 hr. Even a slight intervention such as sealing the X-ray capillaries in which the crystals grow shortens their lifetime drastically (to 6–15 hr).

Since these crystals grow from methanol and/or other alcohols at 4–7° C, cooling to subzero temperatures while collecting crystallographic data is possible and yields patterns of better resolution than those obtained at room temperature. Crystals cooled to about −2° C survive the synchrotron radiation beam for twice as long as at 4° C. Furthermore, the sharp decay of the diffraction intensities at about 20 Å resolution in their diffraction patterns is not as severe as at higher temperatures.

The current crystals diffract to 13 Å resolution at best (typically 18 Å). They last about 3–12 hr in the synchrotron beam permitting about 10–35 photographs, for 5–15 min each, to be taken. Thus, almost a third of a complete crystallographic data set have been collected from a single crystal.

Still photographs of crystals aligned with their long axes parallel or perpendicular to the incident beam displayed easily interpretable Laue circles. Small angle rotation photographs were taken from each zone (Fig. 7.1). The unit cell dimensions for crystals of both the NCA and 799 strains are: $a = 350 \pm 5$ Å, $b = 670 \pm 10$ Å, and $c = 905 \pm 15$ Å, all angles $= 90°$. The *a* axis always corresponded to the long axis of the crystal needle. The extinctions along the 00*l* reciprocal lattice line (clearly seen in Fig. 7.1 b) suggest at least one screw axis in the orthorhombic cell (space group $P222_1$ or $P22_12_1$). Though we propose that the ribosomes are packed in a primitive lattice, the *h*0*l* zone does show extinctions, at least at low resolution, characteristic of a centered lattice ($h + l = 2n$). Identical spacings were observed on patterns from more than ten crystals. Conventional film scanning programs coupled with 25 μ raster scans have already succeeded in indexing diffraction spots and refining the orientation parameters. Thus, all the elements that could assure success of data collection have been demonstrated (Yonath et al., 1986).

The cell parameters determined from electron micrographs of positively stained thin sections from embedded crystals (330 Å × 670 Å × 850 Å) correspond well with the unit cell dimensions determined above by X-ray diffraction (Fig. 7.1). These sections are also similar to those of crystal form 4 (Table 7.1, and in Yonath et al., 1983a; Yonath, 1984) used for image reconstruction studies (Leonard et al., 1982). Both show the ribosomal particles arranged in loosely packed "hexagons" in one section and tightly packed in another section approximately perpendicular to the first. Though a small hexagonal-like cell (450 Å × 405 Å × 256 Å, gamma = 120°) was originally adopted for the image reconstruction study of form 4, a larger, pseudo-orthogonal system can be chosen in the optical diffraction patterns

Table 7.1. Packing Parameters of crystals of ribosomal particles as determined by electron microscopy.

Source	Crystal Type	Crystal Form	Å Cell dimensions	Comments	References
70S *E. coli*	3D		$340 \times 340 \times 590$ $\gamma = 120°$	$P6_3$	a
50S *Halo-bacterium*	3D	1	310×350 $\gamma \times 105°$		b
	3D	2	147×181 $\gamma = 92°$	suitable for X-ray analysis	c
50S *B. stearo-thermo-philus*	3D	1	130×254 $\gamma = 95°$		d
	3D	2	156×288 $\gamma = 97°$		e
	3D	3	260×288 $\gamma = 105°$		e
	3D	4	$405 \times 405 \times 256$ $\gamma = 120°$		e
	3D	5	$213 \times 235 \times 315$ $\gamma = 120°$		f
	3D	6	$330 \times 670 \times 850$ $\gamma = 90°$	X-ray results: $350 \times 670 \times 905$ Å, orthorhombic	g
	2D	ethanol	145×311 $\gamma = 89°$	P2	h
	2D	$(NH_4)_2SO_4$	148×360 $\gamma = 94°$	$P2_1$	i

[1] References: a, Wittmann et al., 1982; b, Shevack et al., 1985; c, Shevack, Shoham, Saper, Wittmann and Yonath, unpublished; d, Yonath et al., 1980; e, Yonath et al., 1983a; f, Yonath et al., 1983b; g, Yonath et al., 1986; h, Arad et al., 1984a; i, Arad et al., 1984b.

of the micrograph (Fig. 7.1) with cell dimensions that agree with our X-ray diffraction patterns. Deviations from orthogonality in the micrograph may reflect the actual packing but also may be due to nonisotropic shrinkage during embedding or may be a consequence of the sectioning angle.

Detected on several single crystal diffraction patterns are sharp arcs or rings, often containing distinct spots, with characteristic spacings of 3.5 Å, 7.0 Å, 8.5 Å, 9.9 Å, 10.8 Å, and 12.5 Å, similar to those previously reported for gels of ribosomes and extracted rRNA (Zubay and Wilkins, 1960; Klug et al., 1961; Langridge and Holmes, 1962). Also, diffraction patterns from samples containing large numbers of micro-crystals show fairly sharp oriented arcs and rings with similar spacings. For aligned crystals, the average arc length is $\pm 30°$. Such patterns may arise from partial orientation of the nucleic acid component within the particle.

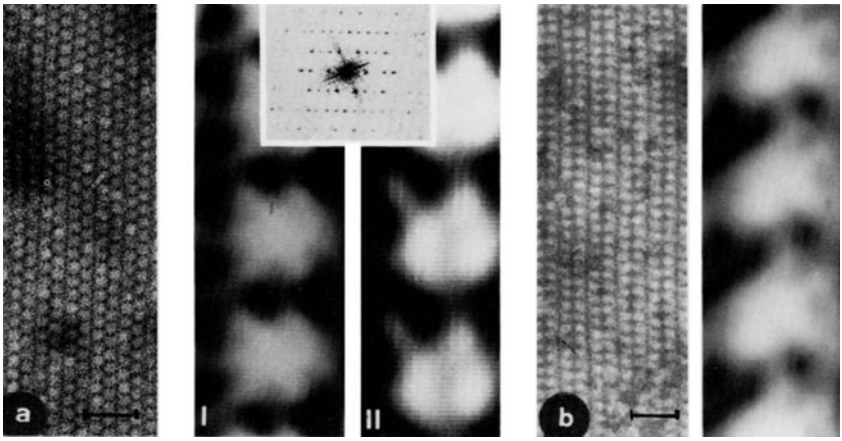

Figure 7.2. a. Electron micrograph of a negatively stained two-dimensional crystalline sheet of the large ribosomal subunit from *B. stearothermophilus* grown at pH 6.0 from 10% ethanol and its optical diffraction pattern. Two filtered images obtained from this pattern at tilt angles of (I) 0° and (II) 25° are shown. Bar length, 500 Å. b. Electron micrograph of a negatively stained two-dimensional crystalline sheet of the large ribosomal subunit from *B. stearothermophilus* grown at pH 6.2 from 2.1 *M* ammonium sulfate and its filtered image. Bar length, 500 Å.

Two-dimensional crystalline sheets that can be visualized directly in the electron microscope have been obtained by essentially the same crystallization method used for the production of the three-dimensional crystals (Fig. 7.2 and in Arad et al., 1984a, b; Leonard et al., 1984). However, in order to obtain sheets, the relative concentrations of Mg^{2+} to 50S particles has to be 500–1000-fold higher than that needed for growth of three-dimensional crystals. Also, only active, pure preparations of the 50S subunits from which either poor or no three-dimensional crystals detectable by light microscopy have been obtained yielded large two-dimensional sheets.

In order to characterize the factors that are responsible for the production of two-dimensional sheets, we have investigated the formation of three-dimensional crystals as a function of the Mg^{2+} concentration in the crystallizing drop. 50S preparations that in low Mg^{2+} concentrations produce normal three-dimensional crystals were tested for crystal growth over a range of Mg^{2+} concentrations. It was found that when the Mg^{2+} concentration in the crystallization medium exceeds 50 m*M*, in most cases no three-dimensional crystals could be detected by light microscopy. Only in a few experiments were small three-dimensional crystals produced, but these dissolved within 1–2 days.

Besides the dependence on Mg^{2+} concentration, the growth conditions of the three-dimensional crystals differ from those of the two-dimensional sheets in the following aspects: In contrast to the three-dimensional crystals

that grow from a variety of alcohols, the two-dimensional sheets are obtained exclusively from ethanol, from which no large three-dimensional crystals could be grown. Also, the three-dimensional crystals are obtained over a wide pH range (with optimum at pH 7.8–9.2), whereas the two-dimensional sheets are produced only over the pH range 5.8–6.8 (with optimum at pH 6.0–6.4). At lower pH values (5.4–5.6), a slight tendency for formation of pyramidlike microcrystals has been observed, and at higher pH values (>7.0) no sheets could be detected.

Recently, for the first time, two-dimensional sheets of ribosomal particles have been obtained using ammonium sulfate instead of alcohols (Fig. 7.2). These sheets have relatively small unit cells (148 Å × 360 Å) consistent in dimensions with forms 1 and 2 of the three-dimensional crystals (Table 7.1 and in Yonath, 1984), are very well ordered (clear twofold screw axis), and diffract optically to a high resolution (about 25 Å).

The current model of overall structure of the large ribosomal subunit was reconstructed at 32 Å resolution from about 45% of optical diffraction data of tilted images of negatively stained sheets. It is consistent in size and shows some of the surface features that have been described previously for this subunit (see, for reviews, Chambliss et al., 1980; Wittmann, 1983). However, the L7/L12 "stalk" appears as a short rod. It is conceivable that it was not resolved in our studies or that the particles undergo conformational changes as a result of either the crystallization process or the preparation for electron microscopy of individual particles. In order to obtain at least indirect evidence for the integrity of the ribosomal particles in the sheets, we have tested the biological activity and the migration profile of the crystallizing drops. It has been found that particles subjected to crystallization conditions for 1–3 weeks co-migrated with standard particles and that almost full activity is preserved in the crystallizing drops. Unfortunately, only a small fraction of the particles in the drop actually comprise the two-dimensional sheets. Therefore, they cannot be separated from the rest of the drop. Thus, there is still some ambiguity concerning the exact nature of the organized particles.

Positively stained thin sections of embedded three-dimensional crystals have been used to obtain packing information, as well as for three-dimensional reconstruction of selected parts of the particles. Cell parameters have been determined for six crystal forms (Yonath et al., 1982a, b; Yonath, 1984) using optical diffraction patterns of electron micrographs of sections in various directions. In most cases the cell dimensions are relatively small (Table 7.1). Three-dimensional image reconstruction studies were performed on a tilt series of uranyl acetate positively stained thin sections of embedded crystals of each of crystal forms 1–4 (Leonard et al., 1981, 1982). Owing to the stability of these sections in the electron beam, up to 80 tilted images could be obtained for each view (about 20 images from four different tilt axes). Thus, the resulting stain distribution maps are clear and reliable. An example is shown in Figure 7.3. Although differently packed, all four forms examined show essentially the same stain

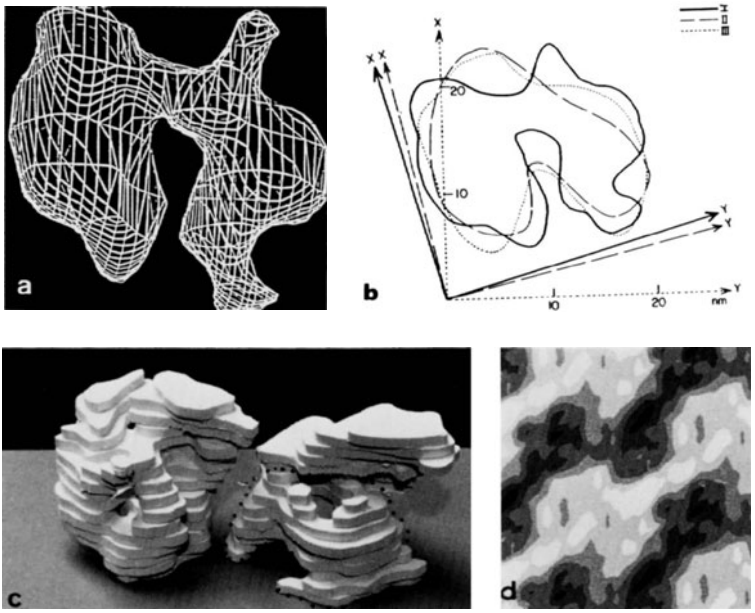

Figure 7.3. a. Computer graphic display of the outline of the stain distribution of crystal form 1 (Yonath, 1984). Contouring level is 3 standard deviations of the entire map. b. Superposition of the overall stain distribution in crystals of forms 1, 2, and 3, in relation to their orientations within the unit cells. c. The three-dimensional model of the stain distribution of the entire unit cell of crystal form 4. The volume of the reconstructed density fits well with that of four large ribosomal subunits, related by a pseudo-twofold rotation axis. The outline of one of the subunits is marked. d. Projected view of the reconstructed stained density of the entire map.

distribution within the particle (Fig. 7.3). The model obtained from these studies is of a size similar to that obtained by other physical techniques (for reviews see Chambliss et al., 1980; Wittmann, 1983) and consists of two domains of unevenly distributed density, which may result from preferential contrast of selected parts (presumably the rRNA) of the ribosomal subunit by the positive stain (Fig. 7.3). Preliminary results from X-ray diffraction patterns indicate partial orientation (presumably in double helices) of some of the rRNA within the particle.

A reconstructed model of the stain distribution within the ribosomal particle has also been obtained using sections of crystal form 4, positively stained with a combination of uranyl acetate together with phosphotungstic acid. Comparison of this model with the one described above shows that the portion of the subunit that interacts with uranyl acetate is distributed mainly in the core of the particle, whereas the ribosomal components that interact with phosphotungstic acid (presumably the proteins) are located closer to the surface and are involved in interactions between the crystalline particles.

Preliminary attempts for detailed comparison of the models obtained from the differently oriented crystal forms and from the different particles within each unit cell are currently in progress. We also plan to use a similar approach to locate the stain density obtained from the positively stained thin sections, within the model that will be obtained from image reconstruction of the negatively stained two-dimensional sheets.

50S Ribosomal Subunits from *Halobacterium marismortui*

Large ($0.4 \times 0.4 \times 0.1$ mm) plate-shaped crystals of the 50S ribosomal subunits from *H. marismortui* have recently been obtained at room temperature as well as at 4° C, using polyethyleneglycol (Fig. 7.4, Table 7.1, and

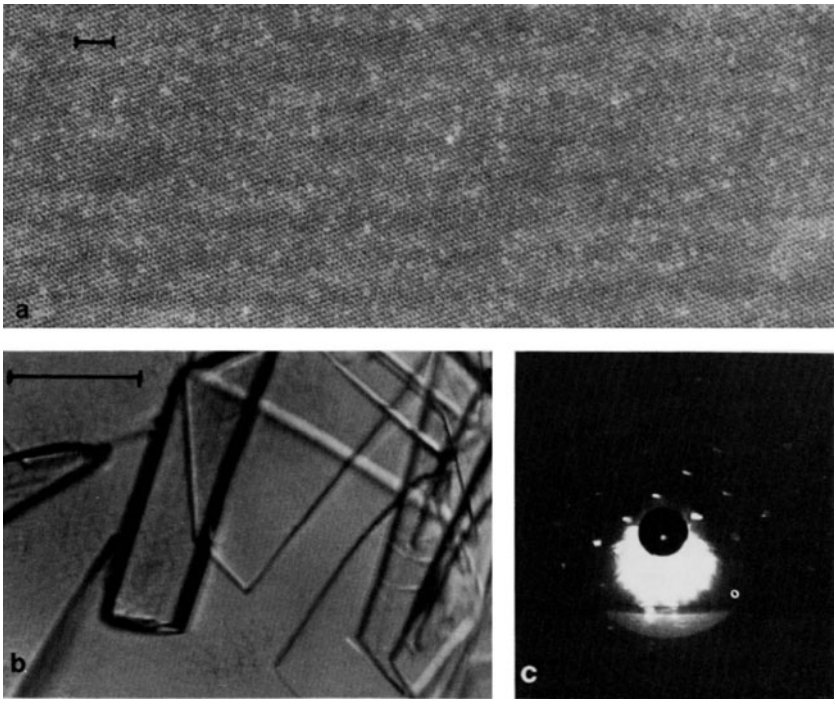

Figure 7.4. Crystals of the 50S ribosomal particles from *H. marismortui* grown at 19 °C from 7% polyethyleneglycol (8000) in the presence of 1.2 *M* potassium chloride, 0.5 *M* ammonium chloride, 0.2 *M* magnesium chloride, 20 m*M* acetate buffer, pH 5.2. Bar length, 0.2 mm. b. Electron micrograph of a positively stained thin section of an embedded crystal, as shown in (a). Bar length, 1000 Å. c. A 0.2° rotation X-ray diffraction pattern of a fragment of a crystal shown in (a) obtained with synchrotron beam at CHESS/Cornell U., operated at about 5 GEV and 20 mA, with 0.20 mm aperture, for 5 min at −2° C. Crystal to film distance, 185 mm.

Shevack et al., 1985). The crystals grow within 2–3 days and reach their final size after 4–5 days. At 2° C they are stable in the synchrotron X-ray beam for 8–12 hr, and their preliminary X-ray diffraction patterns show features to about 10 Å resolution (Shevack, Shoham, Saper, Wittmann, and Yonath, unpublished data).

70S Ribosomes from *Escherichia coli*

The three-dimensional crystals of the 70S ribosomes from *E. coli* are still too small to be studied crystallographically. However, they are well ordered and their cell constants have been determined by electron microscopy (Table 7.1 and in Wittmann et al., 1982). Using information from thin sections together with symmetry considerations, we (Arad, Leonard, Wittmann, and Yonath, unpublished observations) could determine the maximum dimension of one direction of the whole ribosome from *E. coli.* This was found to be 185 ± 20 Å, in good agreement with results from other physical methods (for reviews see Chambliss et al., 1980; Wittmann et al., 1983).

Discussion

Growth of ordered crystals indicates clearly that in spite of their inherent flexibility, under appropriate conditions the ribosomal particles assume a stable conformation for periods that are long enough for crystallization. Although these conditions are not physiological, they do not cause disintegration or loss of biological activity. On the contrary, the crystalline material maintains its activity even for several months, in contrast to isolated ribosomes that fall apart within this period. This agrees well with the hypothesis that when prolonged storage of potentially active ribosomes is needed in living organisms (e.g., hibernation), periodic organization occurs in vivo.

All of the three-dimensional crystals and two-dimensional sheets that have so far been obtained in vivo and in vitro are either of the 50S ribosomal subunits or of whole 70S ribosomes. There have been many attempts to crystallize the small subunits, and with the exception of one case in which short helices have been reported (Clark et al., 1979), no three-dimensional crystals or two-dimensional sheets have so far been obtained from these particles. Furthermore, the interparticle contacts within the two-dimensional sheets of whole ribosomes probably involve only the large subunits, as has been shown in the case of the oocytes of the lizard *Lacerta sicula* where the two-dimensional sheets of whole ribosomes are stable even when the small subunits are removed (Kühlbrandt and Unwin, 1980). It is still too premature to determine whether both observations reflect an inherent flexibility of the small subunits and/or a relative rigidity of the large subunits, or whether it is merely a coincidence.

Investigation of the formation of crystals and sheets as a function of the Mg^{2+} concentration show that the production of two-dimensional sheets require Mg^{2+} concentrations that prohibit growth of three-dimensional crystals. Thus, the intraplane contacts are either indifferent to or even enhanced by the presence of Mg^{2+}, whereas the interplane contacts are subjected to a strong competition with Mg^{2+}. The chemical properties of the two types of contacts are still unknown; the competition with Mg^{2+} may be very specific or may only be an indication for weaker interactions. This finding and the correlation between crystallizability and integrity of rRNA suggest that several interparticle contacts in the crystals involve RNA. Thus, one may conclude that some of the ribosomal RNA is located on the surface of the particle in a favorable position for interparticle contacts.

Some of the three-dimensional crystals and all the two-dimensional sheets are closely packed in relatively small unit cells. However, the largest three-dimensional crystals obtained so far are loosely packed in particular views. A similar "open" arrangement has been observed for most of the in vivo formed crystalline sheets, e.g., lizard ribosomes (Kühlbrandt and Unwin, 1982). This may result from the formation of specific favorable contacts common to particles from several sources but may also be a coincidence.

Among the various crystallization agents that have systematically been examined, in our laboratory as well as in others (Clark et al., 1979, 1982), two-dimensional sheets and three-dimensional crystals of bacterial ribosomes have almost exclusively been grown from organic solvents. Low molecular weight alcohols, which are the best crystallizing agents, may bind specifically to the particles (Miskin et al., 1970) and therefore may give rise to relatively strong crystal contacts. There are currently two exceptions: three-dimensional crystals of the large ribosomal subunits from *H. marismortui,* which have been obtained recently using polyethleneglycol as a precipitant (Shevack et al., 1985), and two-dimensional sheets of the 50S subunits from *B. stearothermophilus,* which have been grown from ammonium sulfate (Arad et al., 1984b). Many technical difficulties with alcohol-grown crystals, such as handling, data collection, and derivation, could be avoided if the crystals are grown from these alternative precipitants.

Our crystallization experiments provide an excellent system for direct investigation of nucleation of crystal growth since the individual particles are large enough to be seen by electron microscopy. For this purpose, crystallization experiments have been interrupted in early stages, and the content of the crystallization solutions has been visualized by electron microscopy. It was observed that the process of growth starts soon after setting up the crystallization experiments, with the formation of aggregates. These, in turn, undergo a rearrangement toward the creation of nucleation centers (Fig. 7.5). The nature and the quality of the expected crystals are dictated by the shape and the degree of order of the nuclei (Yonath et al., 1982b).

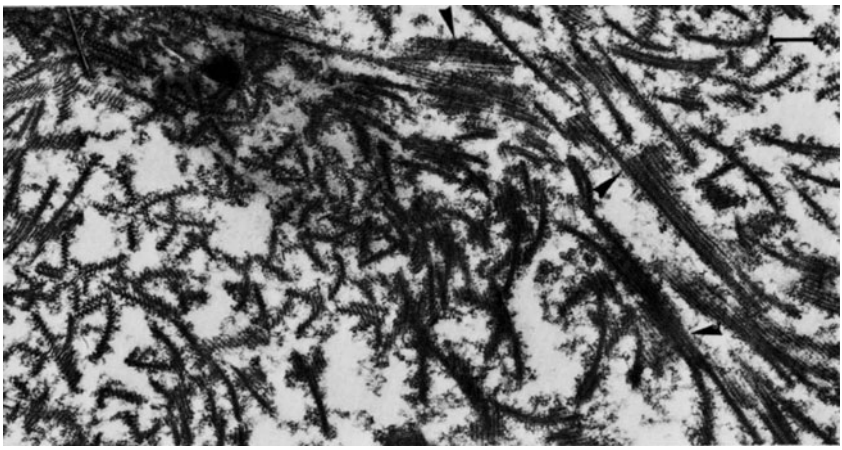

Figure 7.5. An electron micrograph of a thin section of an embeddd crystallization droplet of the 50S ribosomal subunits from *B. stearothermophilus*. Crystallization conditions: 30% methanol, pH 6.3. The experiment was interrupted after 15 days. "Proper" crystals are marked by arrows. Bar length, 5000 Å.

In this chapter we describe the crystalline systems that have been obtained in our laboratory and show that our present crystals are suitable for structural studies. We believe that in spite of the complexity of this system, the limitations and the expected difficulties, we shall be able to obtain high-quality crystallographic data and simultaneously to minimize the inherent limitation of image reconstruction from this sections, by sectioning several crystal forms in different orientations. Progress of the structural studies hinges on the correlation of the crystallographic data with electron microscopic results: The packing and the orientation of the particles within the unit cells can be determined (e.g., Finch et al., 1977; Johnson and Hollingshead, 1981) and preliminary phase information (Podjarny and Moras, unpublished) may be extracted. We plan to coordinate X-ray crystallography and electron microscopy with image analysis and to combine the structural data with the immense amount of biochemical knowledge available on ribosomes. In the first stage we expect to obtain an intermediate reliable model at about 15 Å resolution of the large ribosomal subunit, in which selected components such as proteins, antibiotic- and Fab-binding sites, and specific reactive groups, are unambiguously located. At later stages we will combine information from our initial intermediate model with high-resolution information obtained from crystallographic studies of isolated individual ribosomal components for iterative phase determination by molecular replacement methods. Such data are now or will soon be available for several isolated ribosomal proteins as well as RNA chains (Abdel-Meguid et al., 1983; Appelt et al., 1979, 1981, 1983a–c, 1984; Leijonmarck et al., 1980; Liljas and Newcomer, 1981; Moore et al., 1983; Morikawa 1984; White et al., 1983; Wilson et al., sub-

mitted; Shoham and Reinhardt, unpublished observations). Thus, the determination at this resolution is significant not only in its own rights, but because of its expected contribution to the elucidation of the structure of ribosomes at the molecular level, the long-term goal of our studies.

Acknowledgments

We wish to thank Drs. H.D. Bartunik, K.S. Bartels, J.A. Helliwell, M. Papiz, E. Towns, K. Moffat, and W. Schildcamp for help and collaboration at synchrotron radiation facilities; Dr. K.R. Leonard for intensive image reconstruction studies; Drs. M. Koch, F.L. Hirshfeld, J.L. Sussmann, M. Shoham, B. Shaanan, and W. Traub for continuing interest and for stimulating discussions; and H.S. Gewitz, J. Müssig, J. Piefke, I. Makowski, B. Hennemann, A. Shevack and T. Arad for skillful technical assistance.

References

Abdel-Meguid, S.S., Moore, P.B., Steitz, T.A. (1983). Crystallization of a ribonuclase-resistant fragment of *E. coli* 5S ribosomal RNA and its complex with protein L25, J. Mol. Biol. 171:207–215.

Appelt, K., Dijk, J., Epp, O. (1979). The crystallization of protein BL17 from the 50S ribosomal subunit of *B. stearothermophilus*. FEBS Lett. 103:66–70.

Appelt, K., Dijk, J., Reinhardt, R., Sanhuesa, S., White, S.W., Wilson, K.S., Yonath, A. (1981). The crystallization of ribosomal proteins from the 50S subunit of the *E. coli* and *B. stearothermophilus* ribosome. J. Biol. Chem. 256:11787–11790.

Appelt, K., Dijk, J., White, S.T., Wilson, K.S., Bartels, K. (1983a). Proteins of the *B. stearothermophilus* ribosome: A low resolution crystal analysis of protein L30. FEBS Lett. 160:72–74.

Appelt, K., Dijk, J., White, S.T., Wilson, K.S. (1983b). Proteins of the *B. stearothermophilus* ribosome: crystallization of protein L6. FEBS Lett. 160:75–77.

Appelt, K., White, S.T., Wilson, K.S. (1983c). Proteins of the *B. stearothermophilus* ribosome: crystallization of proteins L30 and S5. J. Biol. Chem. 258:13328–13340.

Appelt, K., Tanaka, I., White, S.T., Wilson, K.S. (1984). Proteins of the *B. stearothermophilus* ribosome: the crystal structure of L6 at 6 Å resolution. FEBS Lett. 165:43–45.

Arad, T., Leonard, K.R., Wittmann, H.G., Yonath, A. (1984a). Two-dimensional crystalline sheets of *B. stearothermophilus* ribosomal particles. EMBO J. 3:127–131.

Arad, T., Leonard, K.R., Wittmann, H.G., Yonath, A. (1984b). Three-dimensional reconstruction studies of 50S ribosomal particles. Fourth International Congress on Electron Microscopy, p. 1459.

Barbieri, M. (1979). Ribosome crystallization in homogenates and cell extracts of chick embryos. J. Supramol. Struct. 10:349–357.

Clark, M.W., Hammons, M., Langer, J.A., Lake, J.A. (1979). Helical arrays of *E. coli* small ribosomal subunits produced in vitro. J. Mol. Biol. 135:507–512.

Clark, M.W., Leonard, K., Lake, J.A. (1982). Ribosomal crystalline arrays of large subunits from *E. coli*. Science 216:999–1001.

Chambliss, G., Craven, G.R., Davies, J., Davis, K., Kahan, L., Nomura, M. eds. (1980). Ribosomes: structure, function and genetics. University Park Press, Baltimore.

Finch, J.T., Lutter, L.C., Rhodes, D., Brown, R.S., Rushton, B., Levitt, M., Klug, A. (1977). Structure of the nucleosome core particles of chromatin. Nature 269:29–41.

Johnson, J.E., Hollingshead, C. (1981). Crystallographic studies of cowpea mosaic virus by electron microscopy and X-ray diffraction. J. Ultrastruct. Res. 74:223–231.

Klug, A., Holmes, K.C., Finch, J.T. (1961). X-ray diffraction studies on ribosomes from various sources. J. Mol. Biol. 3:87–100.

Kress, Y., Wittner, M., Rosenbaum, R.M. (1971). Sites of cytoplasmic ribonucleoprotein-filament assembly in relation to helical body formation in axenic trophozoites of Entamoeba histolytica. J. Cell Biol. 49:773–784.

Kühlbrandt, W., Unwin, P.N.T. (1982). Distribution of RNA and protein in crystalline eukaryotic ribosomes. J. Mol. Biol. 156:431–448.

Lake, J.A., Slayter, H.S. (1972). Three-dimensional structure of the chromatoid body helix of Entamoeba invadens. J. Mol. Biol. 66:271–282.

Langridge, R., Holmes, K.C. (1962). X-ray diffraction studies of concentrated gels of ribosomes from *E. coli*. J. Mol. Biol. 5:611–617.

Leijonmarck, M., Eriksson, S.,Liljas, A. (1980). Crystal structure of a ribosomal component at 2.6 Å resolution. Nature 286:824–826.

Leonard, K.R., Arad, T., Tesche, B., Erdmann, V.A., Wittmann, H.G., Yonath, A.E. (1981). Electron microscopy and three-dimensional reconstruction of 50S ribosomal subunits from the thin sections of crystals. 7th EMBO Symposium, Heidelberg, Abstract.

Leonard, K.R., Arad, T., Tesche, B., Erdmann, V.A., Wittmann, H.G., Yonath, A.E. (1982). Crystallization, electron microscopy and three-dimensional reconstruction studies of ribosomal subunits. In: Electron Microscopy 1982. vol. 3. Offizin Paul Hartung, Hamburg, pp. 9–15.

Leonard, K.R., Arad, T., Wittmann, H.G., Yonath, A.E. (1984). Structural studies on ribosomal particles. Eight Intern. Congress of Biophysics, Abstract.

Liljas, A., Newcomer, M.E. (1981). Purification and crystallization of a protein complex from *B. stearothermophilus*. J. Mol. Biol., 153:393–398.

Marikowa, K. (1984). X-ray diffraction and electron microscopic study of 5S rRNA crystal. Eleventh Intern. Congress on Crystallography, Hamburg, Abstract.

Milligan, R.A., Unwin, P.N.T. (1982). In vitro crystallization of ribosomes from chick embryos. J. Cell. Biol. 95:648–653.

Miskin, R., Zamir, A., Elson, D. (1970). Inactivation and reactivation of ribosomal subunits: the peptidyl transferase activity of the 50S subunit of *E. coli*. J. Mol. Biol. 54:355–378.

Moore, P.B., Kime, M.J., Leontis, N.B., Abdel-Meguid, S.S. (1983). Physical studies on a nucleoprotein from the ribosome of *E. coli*. J. Biomol. Struct. Dynam. 1:383–388.

O'Brien, L., Shelley, K., Towfighi, J., McPherson, A. (1980). Crystalline ribosomes are present in brains of senile humans. Proc. Natl. Acad. Sci. USA 77:2260–2264.

Saper, M.A., Yonath, A., Wittmann, H.G. (1985). X-ray diffraction patterns from single crystals of the large ribosomal subunit from *B. stearothermophilus*. Abstr. Internat. Meeting on Ribosomes. Port Aransas, Texas.

Shevack, A., Gewitz, H.S., Henneman, B., Yonath, A., Wittmann, H.G. (1985). Characterization and crystallization of ribosomal particles from Halobacteria marismortui. FEBS Lett. 184:68–71.

Taddei, C. (1972). Ribosome arrangement during oogenesis of Lacerta sicula, Exp. Cell. Res. 70:285–292.

Unwin, P.N.T. (1977). Three-dimensional model of membrane bound ribosomes obtained by electron microscopy. Nature 269:118–122.

Unwin, P.N.T., Taddei, C. (1977). Packing of ribosomes in crystals from the lizard Lacerta sicula. J. Mol. Biol. 114:491–506.

White, S.W., Appelt, K., Dijk, J., Wilson, K.S. (1983). Proteins of the *Bacillus stearothermophilus* ribosome: a 5 Å structure analysis of protein S5. FEBS Lett. 163:73–75.

Wilson, K.S., Appelt, K., Badger, J., Tanaka, I., White, S.W. The crystal structure of an intact ribosomal protein. Submitted for publication.

Wittmann, H.G. (1983). Architecture of prokaryotic ribosomes. Ann. Rev. Biochem. 52:35–65.

Wittmann, H.G., Müssig, J., Gewitz, H.S., Piefke, J., Rheinberger, H.J., Yonath, A. (1982). Crystallization of *E. coli* ribosomes. FEBS Lett. 146:217–220.

Wittmann, H.G., Yonath, A. (1985). Diffraction studies on crystals of ribosomal particles. In: The structure and function of the genetic apparatus, eds. Ts'o, Nicolini, Plenum Press, New York, pp. 177–189.

Yonath, A., Müssig, J., Tesche, B., Lorenz, S., Erdmann, V.A., Wittmann, H.G. (1980). Crystallization of the large ribosomal subunit from *B. stearothermophilus*. Biochem. Internat. 1:428–435.

Yonath, A., Müssig, J., Wittmann, H.G. (1982a). Parameters for crystal growth of ribosomal subunits. J. Cell. Biochem. 19:629–639.

Yonath, A., Khavitch, G., Tesche, B., Müssig, J., Lorenz, S., Erdmann, V.A., Wittmann, H.G. (1982b). The nucleation of crystals of the large ribosomal subunits from *B. stearothermophilus*. Biochem. Internat. 5:629–636.

Yonath, A., Tesche, B., Lorenz, S., Müssig, J., Erdmann, V.A., Wittmann, H.G. (1983a). Several crystal forms of the 50S ribosomal particles of *B. stearothermophilus*. FEBS Lett. 154:15–20.

Yonath, A., Piefke, J., Müssig, J., Gewitz, H.S., Wittmann, H.G. (1983b) A compact three-dimensional crystal form of the large ribosomal subunit from *B. stearothermophilus*. FEBS Lett. 163:69–78.

Yonath, A. (1984). Three-dimensional crystals of ribosomal particles. TIBS 9:227–230.

Yonath, A., Bartunik, H.D., Bartels, K.S., Wittmann, H.G. (1984). Some X-ray diffraction patterns from single crystals of the large ribosomal subunit from *B. stearothermophilus*. J. Mol. Biol. 177:201–206.

Yonath, A., Saper, M.A., Makowski, I., Müssig, J., Piefke, J., Bartunik, H.D., Bartels, K.S., Wittmann, H.G. (1986). Characterization of single crystals of the large ribosomal particles from *B. stearothermophilus*. J. Mol. Biol. 187:633–636.

Zubay, G., Wilkins, M.H.F. (1960). X-ray diffraction studies of the structure of ribosomes from *E. coli*. J. Mol. Biol. 2:105–112.